

# Effect of Backpressure on Ion Current Density Measurements in Hall Thruster Plumes

Mitchell L. R. Walker,\* Allen L. Victor,\* Richard R. Hofer,\* and Alec D. Gallimore†  
*University of Michigan, Ann Arbor, Michigan 48109*

**The effects of facility backpressure and localized electric fields on the measured ion current densities of Hall thrusters are investigated. Langmuir probe measurements are taken in the near-field plasma surrounding a nude Faraday probe, which is located 1 m from the exit plane of the University of Michigan/U.S. Air Force Research Laboratory P5 Hall thruster. The thruster is operated at an anode flow rate of 5.30 mg/s, at backpressures of  $1.5 \times 10^{-3}$  Pa ( $1.1 \times 10^{-5}$  torr) and  $4.8 \times 10^{-4}$  Pa ( $3.6 \times 10^{-6}$  torr), corrected for xenon. The effect of the facility backpressure is clearly seen in the wings of the plume. A combination of charge-exchange collisions and vacuum chamber gas ingestion into the thruster is believed to be the cause of this phenomenon. The Langmuir probe results indicate that the electric fields near the nude Faraday probe are functions of facility backpressure and the angle from the thruster centerline. The plasma potential measured within 20 mm of the probe varied by no more than 3 V. Thus, the electric fields near the nude Faraday probe are not large enough to explain the increased collection of charge-exchange ions at elevated facility background pressures and large angles from the thruster centerline.**

## Introduction

THE Hall effect thruster's (HET's) combination of high specific impulse, efficiency, and thrust density has increased its popularity for use as spacecraft propulsion. As the availability of in-space power increases, the trend in HET development is growing proportionally toward high-power engines. In the last 10 years, the HET community has seen the completion of flight qualification to western standards of the stationary plasma thruster SPT-100 (1.35 kW) (Refs. 1 and 2), on-going activities for qualifying the SPT-140 (4.5 kW) (Refs. 3 and 4), bipropellant thruster (BPT)-4000 (3 and 4.5 kW) (Ref. 5), and a 1000-h test of the T-220 (10 kW) (Refs. 6 and 7). The latest trends at government laboratories sponsoring HET research are toward power levels of 50–100 kW (Ref. 8). Jankovsky et al. have recently tested a nominally 50-kW engine,<sup>8</sup> and Beal et al. have performed extensive testing on a cluster of four low-power HETs,<sup>9</sup> with the eventual goal of testing high-power clusters. The ability of high-power HETs to perform orbit raising as well as stationkeeping maneuvers may eliminate the need for chemical rockets on satellites and deep-space probes.

Currently, the widespread use of HETs is hindered by a limited understanding of plume interaction with the spacecraft. The plume contains high-speed ions that can erode sensitive spacecraft surfaces, and contamination products created by thruster discharge channel erosion can coat solar cell optics, thus reducing their performance. The parasitic facility effects present in ground tests create additional plume components such as slow propellant ions and neutral atoms.<sup>10</sup> Ions and neutrals present in the HET plume interact through the process of resonant charge exchange (CEX) collisions.

Accounting for CEX ions is not the only obstacle to using ground tests for in-space performance prediction. The wide range of facilities used in Hall thruster testing makes it difficult for researchers

to compare data sets, given dissimilar probe designs and elevated background pressures in facilities with modest pumping speeds and varying geometries.<sup>11</sup>

To this end, an investigation has been launched seeking to understand facility effects introduced by elevated background pressures. This investigation has thus far included the characterization of the performance of the P5 HET at different pumping speeds,<sup>12</sup> an evaluation of a collimated Faraday probe's ability to filter out CEX ions while measuring the ion current density at elevated background pressures,<sup>13,14</sup> and a pressure map of the large vacuum test facility (LVTF) and NASA John H. Glenn Research Center's Vacuum Facility 12 in conjunction with a computational facility model using the direct simulation Monte Carlo method to characterize chamber background pressure of the former.<sup>15</sup> This paper presents Langmuir probe measurements made in the vicinity of a Faraday probe to investigate the formation of electric fields near the Faraday probe. The goal of this work is to understand if the electric field can draw low-energy CEX ions to the collector, which may explain the increase in measured ion current density in the plume extremities with increasing facility backpressures.

Several numerical sputtering model codes have been developed to provide adequate predictions of the HET plume's impact on spacecraft. Inputs to such models are typically the ion energy and ion current density distributions, which are experimentally determined at a known radial position as a function of angle with respect to the thruster centerline. Normally, the ion current density distribution is measured with a "nude" Faraday probe.

A shortcoming of nude Faraday probes is that the measured ion current density depends partly on the facility size and operating pressure, which makes comparisons between ion current density data collected in different facilities nontrivial. Facility effects due to elevated operating pressures are driven by CEX collisions between directed plume ions and the random background population of neutrals. In resonant CEX collisions, a fast moving ion exchanges an electron with a slow moving neutral. Because the process does not involve momentum transfer, the resulting products are a fast neutral moving with the original ion's velocity and a slow ion moving in a random direction. The nude Faraday probe is unable to differentiate between ions created in the discharge chamber and slow CEX ions.

This study investigates Faraday probe collector phenomena by interrogating the plasma in the near field of a nude Faraday probe with a Langmuir probe at background pressures above and below  $1.3 \times 10^{-3}$  Pa ( $1.0 \times 10^{-5}$  torr). Randolph et al. suggest that facility effects on Hall thruster plume measurements are severe above  $1.3 \times 10^{-3}$  Pa ( $1.0 \times 10^{-5}$  torr) (Ref. 16). The experimental results

Received 19 January 2004; revision received 23 September 2004; accepted for publication 10 October 2004. Copyright © 2004 by Mitchell L. R. Walker. Published by the American Institute of Aeronautics and Astronautics, Inc., with permission. Copies of this paper may be made for personal or internal use, on condition that the copier pay the \$10.00 per-copy fee to the Copyright Clearance Center, Inc., 222 Rosewood Drive, Danvers, MA 01923; include the code 0748-4658/05 \$10.00 in correspondence with the CCC.

\*Graduate Student Researcher, Plasmadynamics and Electric Propulsion Laboratory, Department of Aerospace Engineering, 1052 FXB Building, 1320 Beal Avenue. Student Member AIAA.

†Professor, Plasmadynamics and Electric Propulsion Laboratory, Department of Aerospace Engineering, 3037 FXB Building, 1320 Beal Avenue. Associate Fellow AIAA.

and discussion of plasma parameters obtained by the Langmuir probe are presented. A discussion of the relationship between the measured plasma parameters and the Faraday probe results then follows.

## Experimental Apparatus

### Vacuum Facility

All experiments are conducted in the LVTF. The LVTF is a stainless-steel-clad vacuum chamber that has a diameter of 6 m and a length of 9 m. The thruster is mounted at station 1, as indicated in Fig. 1. At this position, the thruster is medially located along the radial axis of the tank, and the plume is allowed to expand freely approximately 7 m along the centerline axis. The facility is equipped with seven CVI TM-1200 reentrant cryopumps, each of which is surrounded by a liquid nitrogen baffle. With seven pumps operating, the pumping speed of the facility is 500,000 l/s for air, and 240,000 l/s for xenon.

Two hot-cathode ionization gauges monitor chamber pressure, as shown in Fig. 1. The first gauge is a Varian model 571 gauge with an HPS model 919 hot cathode controller. The second is a Varian model UHV-24 nude gauge with a Varian UHV senTorr vacuum gauge controller. Pressure measurements from both gauges are corrected for xenon using the known base pressure of air and a correction factor of 2.87 for xenon according to the following equation<sup>17</sup>:

$$P_c = [(P_i - P_b)/2.87] + P_b \quad (1)$$

where  $P_c$  is the corrected pressure on xenon,  $P_b$  is the base pressure, and  $P_i$  is the indicated pressure when xenon is flowing into the vacuum chamber.

### Hall Thruster

The experiments are performed with the U.S. Air Force Research Laboratory/University of Michigan P5 and the NASA-173Mv1 Hall thruster. The P5 has a mean diameter of 148 mm, a channel width of 25 mm, and a nominal power rating of 5 kW. A more detailed discussion of the P5 Hall thruster may be found in Refs. 18 and 19. The P5 and the 173Mv1 have the same discharge channel dimensions, but different magnetic circuit designs.<sup>20,21</sup> A laboratory-model cathode is located at the 2 o'clock position on the P5 and at the 12 o'clock position on the 173Mv1 (Ref. 22). The thrusters are allowed to operate for 2 h after initial exposure to vacuum to allow the discharge channel walls to outgas. The cathode orifice is located approximately 25 mm downstream and 25 mm radially away from the outer front pole piece at an angle of 30 deg from thruster centerline.

High-purity (99.999% pure) xenon is fed to the Hall thruster from compressed gas bottles through stainless-steel feed lines. Anode and cathode propellant flows are controlled and monitored with MKS 1179A mass flow controllers. The flow controllers are calibrated with a custom apparatus that measures gas pressure and temperature as a function of time in an evacuated chamber of known volume. The mass flow controllers have an accuracy of  $\pm 1\%$  full scale.

The thruster is operated at a discharge voltage of 300 V and anode mass flow rates of 4.81 and 5.06 mg/s, corresponding to a discharge currents of approximately 4.35 A. For the experiments reported here, the LVTF is operated at nominal pumping speeds of 70,000 and 240,000 l/s, corresponding to background pressures of  $1.5 \times 10^{-3}$  Pa ( $1.1 \times 10^{-5}$  torr) and  $4.8 \times 10^{-4}$  Pa ( $3.6 \times 10^{-6}$  torr), respectively. A previous study has shown that the nude ion gauge reading is the most accurate estimate of the LVTF's background pressure.<sup>15</sup>

### Probe Design

Figure 2 shows a schematic of the nude Faraday probe. The nude Faraday probe consists of a 2.31-cm-diam collection electrode enclosed within a guard ring. The collection electrode is aluminum, spray coated with tungsten to minimize secondary electron emission. The secondary electron yield of tungsten is approximately 0.02 for ion energies of 200–600 V (Ref. 23). Both the collector and guard ring are designed to be biased to the same negative potential below facility ground to repel ambient electrons and to minimize edge effects around the collector by creating a flat, uniform sheath over the collection area. Table 1 lists the relevant dimensions of the nude Faraday probe.

The guard ring spacing is compared to the plasma debye length to verify qualitatively the collector sheath profile of nude Faraday probe. Reference 19 contains measurements of typical P5 plume parameters. From the measured electron temperature  $T_e$  and the electron number density  $n_e$ , the debye length  $\lambda_d$  is calculated, and the probe sheaths  $t_s$  are approximately 1.5–3.0 mm (sheath thickness 5–10 D lengths). The guard ring gap of the nude Faraday probe is

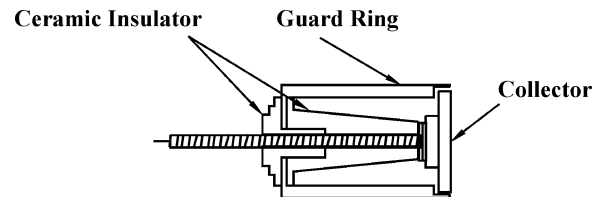


Fig. 2 Schematic of nude Faraday probe, collector isolated from guard ring with ceramic standoffs.

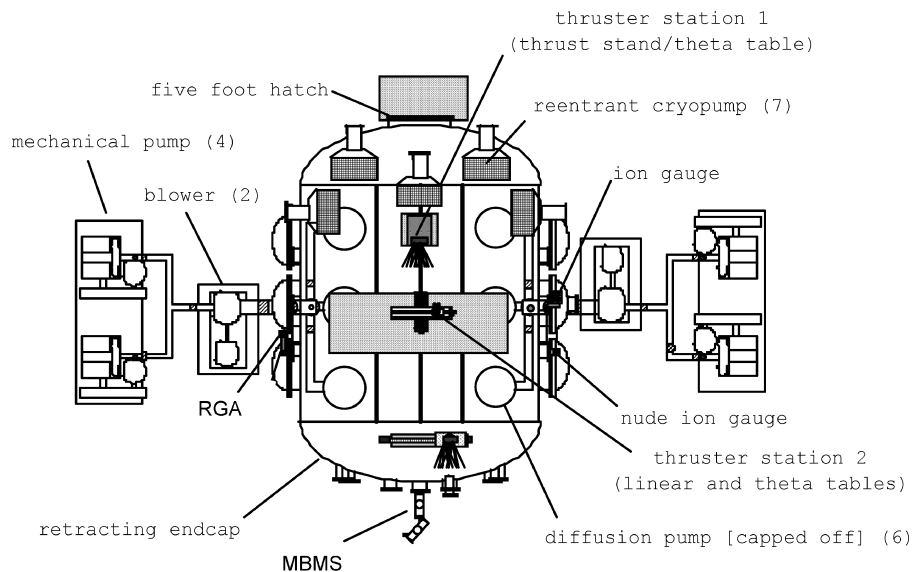


Fig. 1 Schematic of LVTF (not to scale).

0.4 mm, which is smaller than the sheath thickness and should result in a smooth sheath surface over the collector.

### Data Acquisition System

The thruster is mounted with the exhaust beam aligned with the chamber axis, such that the thruster centerline is referenced as 0 deg. The nude Faraday probe is positioned on an overhead, rotating arm that is attached to a rotary table with a repeatability of 12 arc-sec. The probes are aligned to the center of the P5 exit plane and placed  $100.9 \pm 0.1$  cm downstream of the thruster. A scan of the thruster plume from  $-100$  to  $100$  deg, in 1-deg measurement increments, takes approximately 6 min.

Probe data are acquired using a 22-bit, 20-channel data acquisition system. The collector surface and guard ring of the nude Faraday probe are biased 20 V below facility ground by a single power supply. Earlier use of nude probes at the Plasmadynamics and Electric Propulsion Laboratory indicates that a bias voltage of  $-20$  V below facility ground is sufficient for the collector to enter ion saturation without substantial sheath growth.<sup>13,23</sup> The probe current is measured with a  $99.6\text{-}\Omega$  shunt. Typical collector currents range from 0.2 to 3.4 mA.

### Experimental Results

Table 2 lists the studied 173Mv1 operating conditions. In the following discussion, all data reported are with the collector and guard ring of the nude Faraday probe biased to 20 V below facility ground.

The effect of facility backpressure on the measured ion current density of the nude probe is investigated by varying the pumping speed of the LVTF. As the facility backpressure increases, the thruster discharge current increases as more background xenon gas is ingested into the thruster discharge chamber. The anode mass flow rate is adjusted to keep the discharge current constant at all pumping speeds. As shown in Table 2, the magnet settings remain constant at each power setting for both pumping speeds. In Table 2  $I_{ic}$  is the inner magnet current,  $I_{oc}$  is the outer magnet current, and  $V_{c-g}$  is the voltage difference between the cathode and ground.

Figure 3 shows ion current density traces taken with the nude Faraday probe. Figure 4 shows the ion current density percent difference between the two operating backpressures. The points of interest in each of Figs. 3 and 4 are discussed in subsequent sections of this paper.

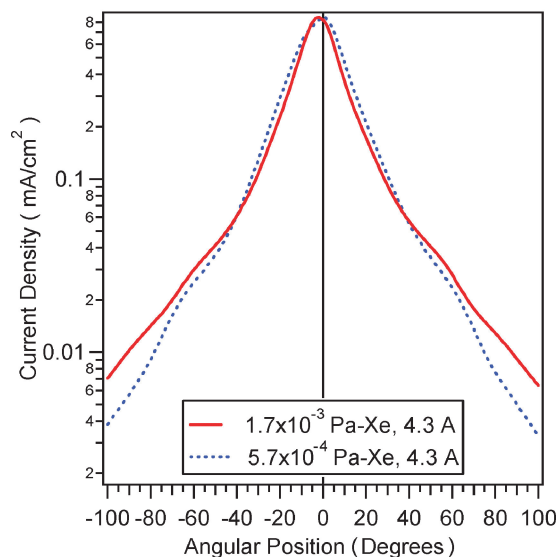
### Discussion

Figure 3 shows ion current density traces at a 173Mv1 operating condition of 300 V and 4.3 A for both backpressures. The effect of the facility backpressure is clearly seen in Fig. 3 in the wings of the plume. Yet, the ion current density profile is not significantly affected within 20 deg of centerline, which may be explained by noting that, on the centerline, the number of slow CEX ions is negligible in comparison to the number of ions born in the discharge channel. Similar results were obtained by Manzella and Sankovic.<sup>24</sup> However, Manzella and Sankovic changed the facility pressure by

bleeding xenon into the test chamber through an auxiliary bleed valve on the tank wall, not by varying pumping speed.

The effect of the CEX ions on Faraday probe measurements is most evident at large angles in the ion current density profiles where the primary-to-CEX ion ratio is small. The effect of CEX ions increases as the facility backpressure increases due to an increase in the number of neutrals atoms present in chamber and, therefore, the high number of CEX collisions within the measurement envelope. The increase in CEX ion number density causes the Faraday probe to measure an ion current density higher than the true value.

The ion current density percent difference between two pumping speeds displays the effect of facility backpressure on ion current density measurements. Figure 4 shows the percent difference in



**Fig. 3** Ion current density vs position for nude Faraday probe at backpressures of  $1.7 \times 10^{-3}$  Pa Xe and  $5.7 \times 10^{-4}$  Pa Xe (300-V, 4.3-A thruster operation).

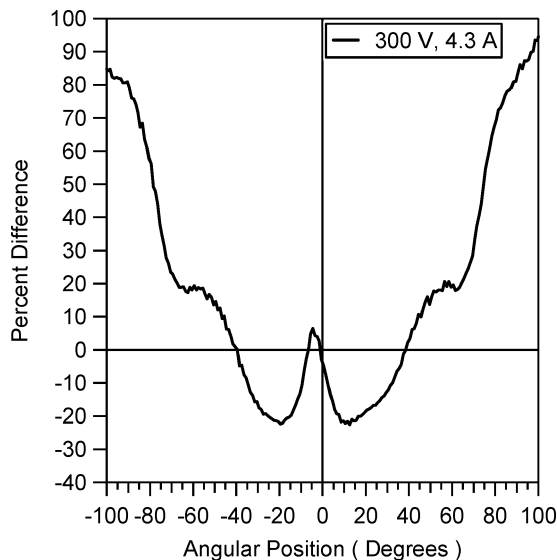


**Fig. 4** Percent difference between current density profiles measured at backpressures of  $1.7 \times 10^{-3}$  Pa Xe and  $5.7 \times 10^{-4}$  Pa Xe using nude Faraday probe at operating condition of 300 V, 4.3 A.

**Table 1** Dimensions of nude Faraday probe

Part name	Dimension, cm
<i>Probe collector</i>	
Outer diameter	2.31
Gap thickness	0.23
<i>Probe guard ring</i>	
Outer diameter	2.540
Thickness	0.074

**Table 2** NASA-173Mv1 operating conditions

Discharge voltage, V	Discharge current, A	Anode flow, mg/s	Cathode flow, mg/s	$I_{ic}$ , A	$I_{oc}$ , A	$V_{c-g}$ , V	Pressure Xe, Pa	Pressure Xe, torr	Probe bias with regard to ground, V
300	4.39	4.81	0.55	2.00	1.50	-11.5	$1.7E-03$	$1.3E-05$	-20
300	4.35	5.06	0.55	2.00	1.50	-11.9	$5.7E-04$	$4.3E-06$	-20

measured ion current density between a back pressure of  $1.7 \times 10^{-3}$  and  $5.7 \times 10^{-4}$  Pa at a 173Mv1 operating condition of 300 V at 4.3 A. As seen in Fig. 4, the difference between measurements taken at  $1.7 \times 10^{-3}$  and  $5.7 \times 10^{-4}$  Pa is approximately 7% on the centerline. The increasing percent difference at large angles from the centerline corresponds to the greater fraction of CEX ions in the plume perimeter.

### Probing a Probe

Figures 3 and 4 show that deviations in ion current density profile increase as the facility backpressure increases for plume angle measurements beyond approximately  $\pm 40$  deg. One possible explanation for the ion current density deviations is that electric fields may form in the local vicinity of the nude Faraday probe due to the negative bias voltage applied to the guard ring and collector.<sup>1</sup> These electric fields may then capture slow CEX ions and draw them into the collector, which would result in an artificially high ion current density measurement. This process may explain the rise in ion current density in the plume extremities as the backpressure increases. An investigation of the electric field near the probe is required to verify its relation to ion collection.

We use a Langmuir probe to interrogate the near-field plasma surrounding the current-collecting nude Faraday probe to help determine the mechanisms that control the Faraday probe collection phenomena. The experiments are conducted in the LVTF using the P5 Hall thruster, which is described in the preceding text. For this portion of the study, the thruster is centered about the chamber centerline, at station 2, as shown in Fig. 1.

The nude Faraday probe is centered on the P5 Hall thruster centerline 1 m downstream of the exit plane and measures the ion current at angles of 40 and 90 deg from the thruster centerline. Figure 4 shows that at 40 deg, the ion current density percent difference between  $1.7 \times 10^{-3}$  and  $5.7 \times 10^{-4}$  Pa is approximately zero. Figure 4 also shows that the ion current density percent difference approaches its maximum at 90 deg. The goal is to measure the electron number density, electron temperature, and plasma potential in the immediate vicinity of the nude Faraday probe to study Faraday probe ion collection phenomena. In addition, these data will be used for verification of numerical simulations and offer guidance on designing improved Faraday probes and/or correction algorithms.

A cylindrical Langmuir probe, manufactured by Hiden, is used to characterize the plasma parameters. The probe tip is constructed of 0.1-mm-diam tungsten and has a length of 7.5 mm. The Langmuir and Faraday probe connections are made with coaxial vacuum feedthroughs at the LVTF wall. The Langmuir probe is oriented such that the collector filament is vertical and perpendicular to the ion beam. The tip of the Langmuir probe collection surface is level with the centerline of the nude Faraday probe and the centerline of the P5 Hall thruster. Two linear translation tables, mounted perpendicular to each other, move the Langmuir probe through the plume. The tables are powered by stepping motors and have an accuracy of  $\pm 0.0025$  mm in each direction. The thruster plume angle is varied by rotating the thruster on the theta table described earlier.

The floating potential, plasma potential, electron temperature, electron density, and ion density are determined at 43 points spaced from 1 to 20 mm away from the nude Faraday probe for each of the test conditions and plume angles. Figure 5 shows the location of each interrogation point with respect to the nude Faraday probe. In addition, three points are taken significantly farther away from the nude Faraday probe, but in the same plane as the other points. Two points are taken 90 mm off of the thruster centerline in the plane of the probe collector. The third point is taken 100 mm in front of the probe collector surface.

The Langmuir probe bias voltage and current measurements are controlled through the Hiden Langmuir probe system.<sup>25</sup> The Hiden software, ESPion, records the data and calculates the plasma characteristics. The current is measured from the probe through the ion saturation region, the electron energy distribution, and the electron saturation region, respectively, by biasing the Langmuir probe from  $-25$  to 30 V. Each Langmuir probe trace contains 1100 points, and 10 sweeps are obtained at each position. The Langmuir probe

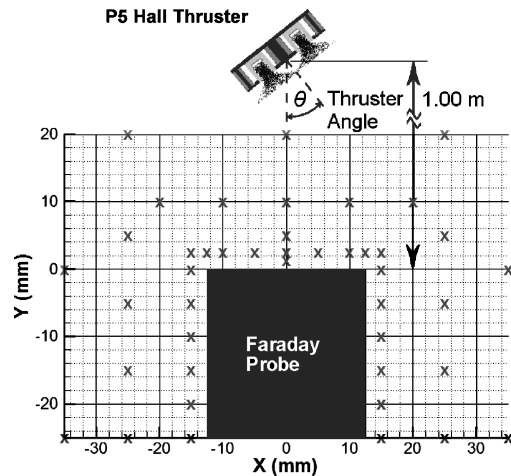


Fig. 5 Schematic of Langmuir probe measurements taken about nude Faraday probe with respect to P5 Hall thruster.

is cleaned by the 200+ eV ions that collide with it. Data collection from the nude Faraday probe is accomplished with the same electrical setup described in the first portion of the text.

### Probing a Probe Results

The thruster is operated at a discharge voltage of 300 V and an anode mass flow rate of 5.30 mg/s, corresponding to a discharge current of 4.86 A. With the collector and guard ring of the nude Faraday probe biased to  $-20$  V, the Langmuir probe characterizes the plasma in the vicinity of the nude Faraday probe. No change is observed in the measured ion current density while the Langmuir probe characterizes each case.

The Hiden software applies orbital-motion-limited (OML) and thin-sheath theory to the resultant Langmuir probe traces to determine several plasma parameters. The use of OML theory for analysis of the data is valid because the probe radius (0.1 mm) is much smaller than the calculated sheath thickness (0.5–0.9 mm and 5–10 debye lengths). In addition, a collisionless sheath may be assumed because the sheath thickness is much smaller than the electron mean free path (approximately 1 m). The Langmuir probe current (1–5 mA) is small with respect to the total discharge current (4.86 A); thus, the probe represents a minor perturbation to the plasma. Therefore, the measurements and analysis are expected to be valid. For standard Langmuir probe theory, it is indicated in Ref. 26 that the electron temperature and ion number density measurements have an uncertainty of 20 and 50%, respectively.

The most notable plasma parameters measured are the electron density, ion density, and plasma potential. The three additional plume measurements taken significantly far away from the nude Faraday probe are used to verify the assumption that large gradients in the plasma parameters do not exist at positions outside of the area of interrogation for the nude Faraday probe.

The electron and ion densities are calculated for several points around the nude Faraday probe for each test condition. Figure 6 shows the electron density measurements along the centerline of the nude Faraday probe at both backpressures and angles from the thruster centerline. Figure 6 shows that the electron density decreases when the facility backpressure increases. The electron density decreases by 74% for the 40-deg plume angle vs a 54% decrease for the 90-deg plume angle as the pressure increases. In the test case, with a background  $4.8 \times 10^{-4}$  Pa ( $3.6 \times 10^{-6}$  torr) at 40 deg, the electron density decreases as the Langmuir probe is moved away from the Faraday probe; however, all other test cases show constant electron density or a slight increase as farther distances from the Faraday probe are interrogated.

Figure 7 shows the ion density vs distances from the nude Faraday probe at both backpressures and angles from the thruster centerline. The ion density increases as the backpressure increases from  $4.8 \times 10^{-4}$  to  $1.5 \times 10^{-3}$  Pa, and the opposite trend is observed with the electrons. At the point closest to the nude Faraday probe,

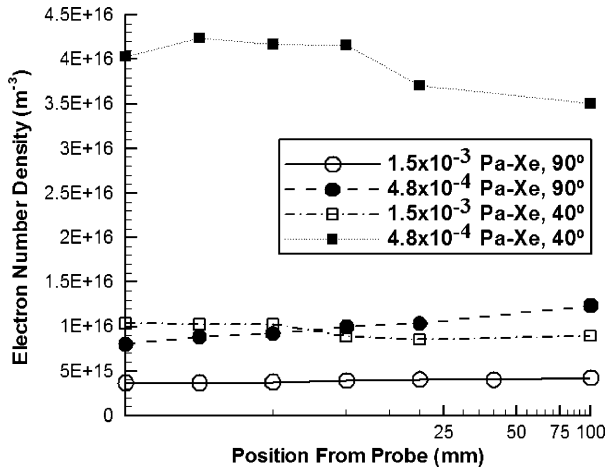


Fig. 6 Electron number density measurements along centerline of nude Faraday probe.

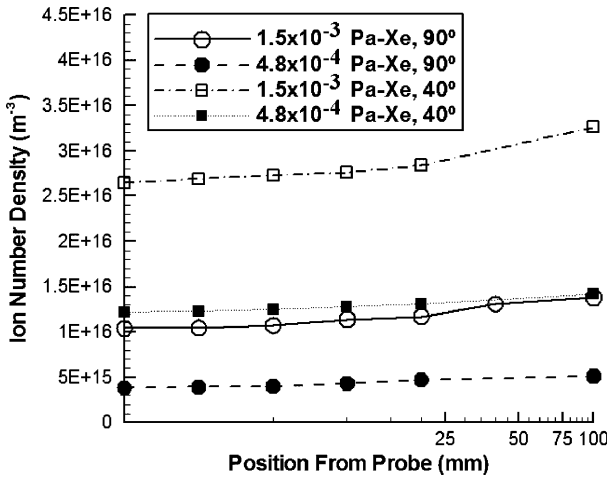


Fig. 7 Ion number density measurements along centerline of nude Faraday probe.

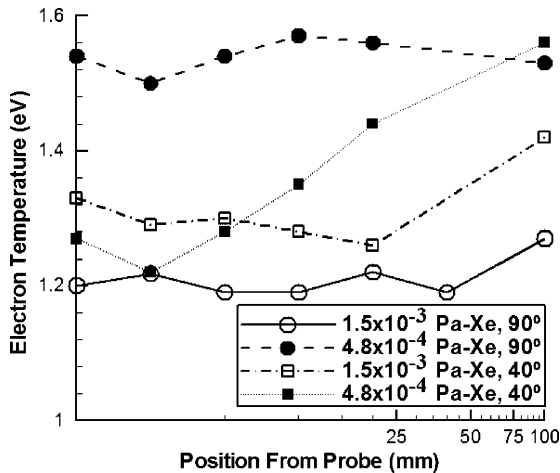


Fig. 8 Electron temperature measurements along centerline of nude Faraday probe.

the ion density increases by 117% for the 40-deg plume angle and 171% for the 90-deg plume angle. The ion density generally increases for all test cases as the Langmuir probe moves away from the nude Faraday probe toward the thruster.

Figure 8 shows the electron temperature along the centerline of the nude Faraday probe. A slight increase in temperature is noticed at further distances for all cases except for the test case with a backpressure of  $4.8 \times 10^{-4}$  Pa at the 90-deg plume angle. In this case, the electron temperature does not vary substantially.

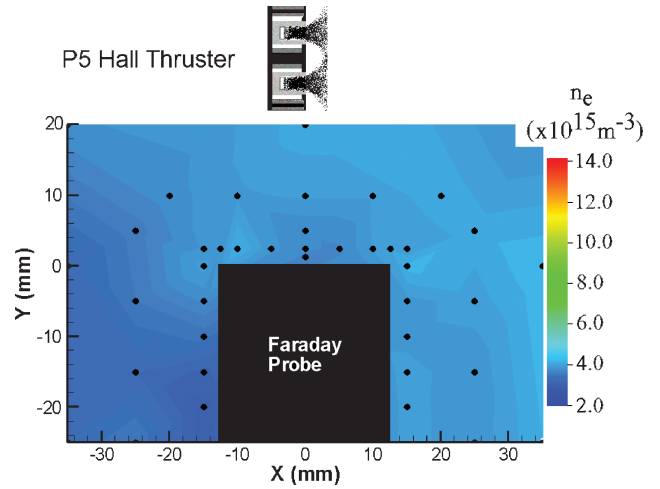


Fig. 9 Electron density measurements at 90 deg at backpressure of  $1.5 \times 10^{-3}$  Pa ( $1.1 \times 10^{-5}$  torr).

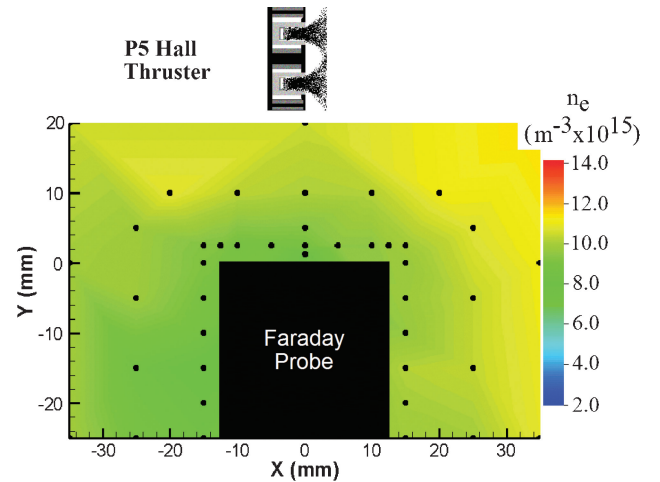


Fig. 10 Electron number density at 90 deg at backpressure of  $4.8 \times 10^{-4}$  Pa ( $3.6 \times 10^{-6}$  torr).

Figures 9 and 10 show the electron density and Figs. 11 and 12 show the ion density at the 90-deg plume angle at different backpressures. The solid black circles indicate the location of each Langmuir probe measurement. Linear triangulation is used to calculate the values between each measurement point. A definite shadowing effect is apparent for both the electron and ion density measurements. The left side of the Faraday probe, farthest from the thruster exit plane, has lower electron and ion number densities.

Figures 13–16 show the plasma potential for each test condition. The plasma potential shows a definite decrease around the nude Faraday probe for both plume angles at the  $4.8 \times 10^{-4}$  Pa backpressure. However, the trend is unclear at the higher backpressure of  $1.5 \times 10^{-3}$  Pa. At 40 deg and the lower pressure from the thruster centerline, there is a slight increase in plasma potential, whereas at 90 deg there is no marked change around the probe. The plasma potential is affected more near the probe for lower facility backpressures.

### Discussion

The Langmuir probe measurements indicate electron number densities in the range of  $10^{15}$ – $10^{16}$   $m^{-3}$ . Haas et al. report electron number densities on the same order of magnitude for similar measurements of the P5 plume.<sup>19</sup> This agreement gives confidence in the Hidden system.

Figures 11 and 12 show that the ion number density near the nude Faraday probe is two–three times higher for a backpressure of  $1.5 \times 10^{-3}$  Pa than for  $4.8 \times 10^{-4}$  Pa. The electric field present

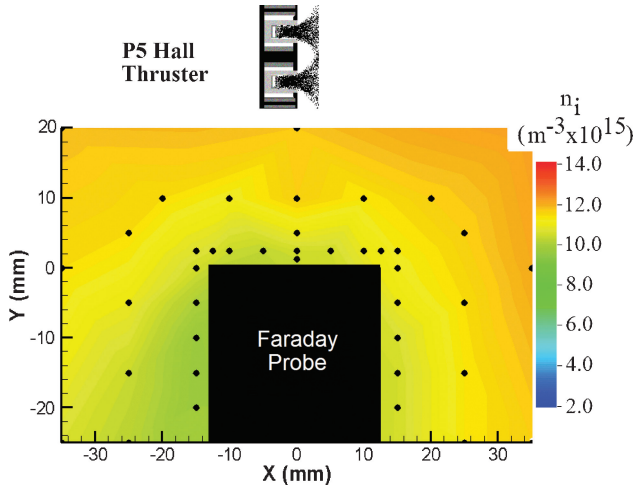


Fig. 11 Ion number density at 90 deg at backpressure of  $1.5 \times 10^{-3}$  Pa ( $1.1 \times 10^{-5}$  torr).

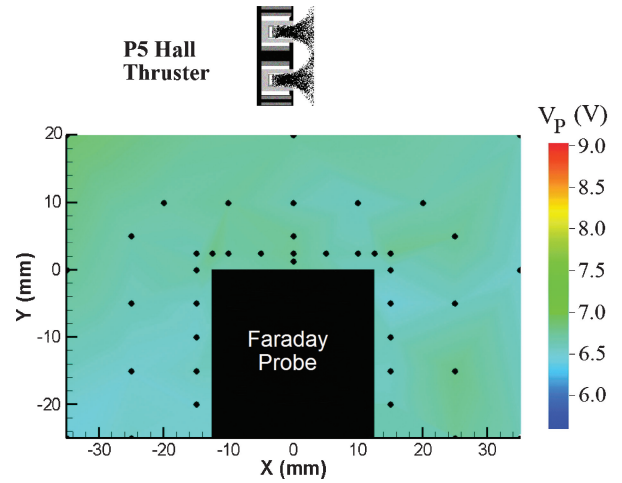


Fig. 13 Plasma potential at 90 deg at backpressure of  $1.5 \times 10^{-3}$  Pa ( $1.1 \times 10^{-5}$  torr).

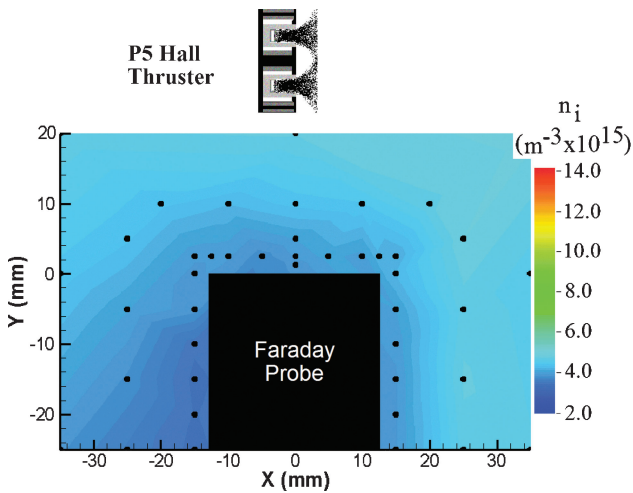


Fig. 12 Ion number density at 90 deg at backpressure of  $4.8 \times 10^{-4}$  Pa ( $3.6 \times 10^{-6}$  torr).

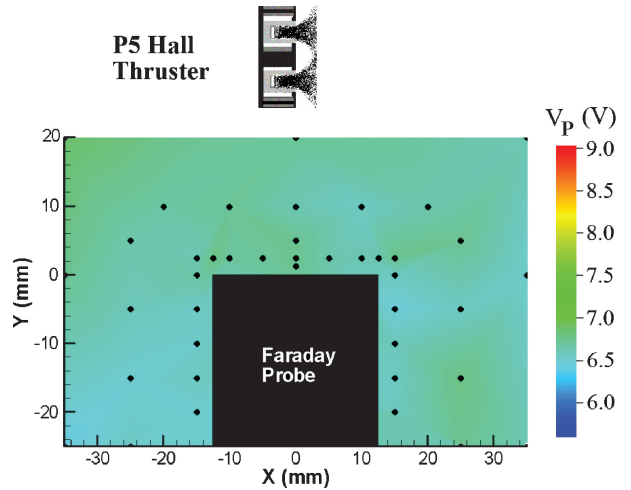


Fig. 14 Plasma potential at 90 deg at backpressure of  $4.8 \times 10^{-4}$  Pa ( $3.6 \times 10^{-6}$  torr).

at a backpressure of  $1.5 \times 10^{-3}$  Pa may be suppressed by the large number of ions around the probe. The factor of increase in ion density at the higher backpressure correlates with the increased current density measured by the Faraday probe. The observation of a larger increase in ion density for higher plume angles is concordant with CEX theory.

Figures 13 and 15 show the presence of a weak electric field near the Faraday probe at a backpressure of  $1.5 \times 10^{-3}$  Pa. The electric field increases in strength and loses symmetry at the lower backpressure of  $4.8 \times 10^{-4}$  Pa, as shown in Figs. 14 and 16. The electric fields surrounding the Faraday probe are not strong enough to pull CEX ions to the collector, which would lead to elevated ion current density measurements, even in the plume extremities where the ratio of CEX to beam ions is large.

Figure 4 shows that the ion current density percent difference between backpressures of  $1.5 \times 10^{-3}$  and  $4.8 \times 10^{-4}$  Pa is 1% at 40 deg and 84% at 90 deg. The 84% difference at 90 deg agrees well with the Langmuir probe data, which show that the ion number density is always greatest at the higher backpressure of  $1.5 \times 10^{-3}$  Pa. For angles of 40 deg to the thruster centerline, the measured ion current density is greatest at the lower backpressure of  $4.8 \times 10^{-4}$  Pa. At a backpressure of  $4.8 \times 10^{-4}$  Pa there are fewer CEX collisions and, hence, more beam ions than at the higher backpressure of  $1.5 \times 10^{-3}$  Pa. Yet, the Langmuir probe indicates that the ion number density is greatest at the higher backpressure.

The percentage of beam ions that reach the Faraday probe and the Langmuir probe is affected by the facility operating pressure. Gulczinski's ion energy distribution measurements of the P5, at

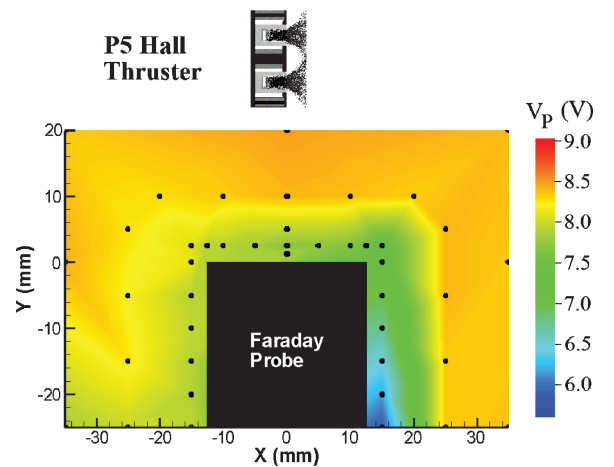


Fig. 15 Plasma potential at 40 deg at backpressure of  $1.5 \times 10^{-3}$  Pa ( $1.1 \times 10^{-5}$  torr).

the 300-V, 5-A operation condition, show that the ion energy of singly charged ions at 40 and 90 deg is approximately 280 and 180 eV, respectively.<sup>27</sup> The percentage of beam ions that reach the Faraday probe and the Langmuir probe without a collision is calculated using the ion energy estimates and the Xe-Xe<sup>+</sup> cross section data in Ref. 28. At 40 deg the beam ion survival rate is 90% for  $1.5 \times 10^{-3}$  Pa and increases to 97% for  $4.8 \times 10^{-4}$  Pa. At 90 deg, the beam ion survival rate is 89% at  $1.5 \times 10^{-3}$  Pa and increases to 96%

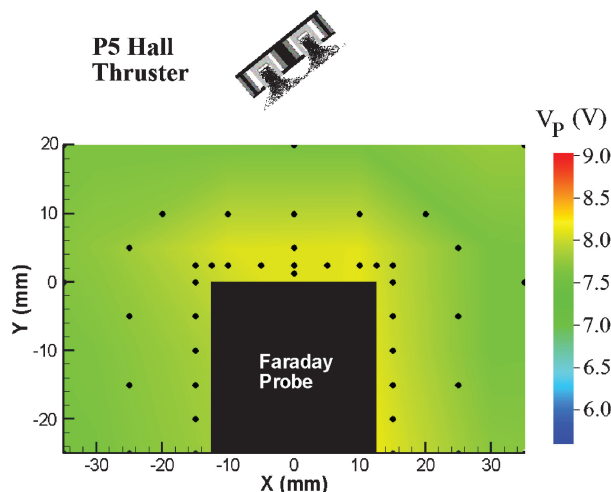


Fig. 16 Plasma potential at 40 deg at backpressure of  $4.8 \times 10^{-4}$  Pa ( $3.6 \times 10^{-6}$  torr).

for  $4.8 \times 10^{-4}$  Pa. The decrease in the number of collisions due to the lower operating pressure of  $4.8 \times 10^{-4}$  Pa only accounts for a small increase in the percentage of ions that reach the probes at 40 deg.

The cylindrically shaped Langmuir probe collects low-energy CEX ions from all directions. It also collects energetic beam ions that make a direct collision with the electrode. In comparison, the Faraday cup only collects current from the disk collector facing the thruster. CEX ions that approach the Faraday probe from the sides or from behind are not collected due to its geometry. Therefore, the Langmuir probe is more susceptible to higher current density measurements due to CEX ions approaching from all sides of the probe at higher pressures. This may explain why the Langmuir probe indicates a higher ion number density for the  $1.5 \times 10^{-3}$  Pa backpressure, whereas the Faraday probe indicates that the ion current density is greatest at the  $4.8 \times 10^{-4}$  Pa backpressure at 40 deg to the thruster centerline. Because the beam survival rate is higher for lower pressures, more beam ions are collected by the Faraday cup, and a higher current density is measured.

A shadowing effect is observed in ion density measurements around the Faraday probe in Figs. 9–12. Ions emanating from near the centerline of the plume created by CEX collisions could be arriving at the probe from the side. This could be a result of the negative potential of the Faraday probe repelling electrons from the face of the probe, as well as the drawing of ions through a forced diffusion process toward the probe.

The plasma potential plots show that the electric field is confined to within a few centimeters of the Faraday probe. The electric field occupies a larger region for the lower backpressures; however, only a variance of approximately 3 V was measured for each of the test cases. Therefore, the trajectories of the beam ions with respect to the Faraday probe (traveling between 180 and 280 eV) are virtually unaffected by the electric field. The contribution to current density from beam ions is unlikely to change for each test case because the electric field is weak around the Faraday probe. However, the increase in current density can be attributed to thermal ions produced by CEX. If a Maxwellian velocity distribution of the thermal energy ions is assumed, a random flux calculation for the current density can be estimated through the ion temperature and density. In Eq. (2),  $c_i$  represents the thermal speed of the ions:

$$j_{\text{rand}} = en_i c_i / 4 \quad (2)$$

Williams et al. observed ion temperatures ranging from 350 to 500 K through laser-induced fluorescence measurements in the plume.<sup>29</sup> If the xenon ion temperature is assumed to be approximately 425 K, and the measured ion densities are approximately  $1 \times 10^{16} \text{ m}^{-3}$  (at 90 deg at a backpressure of  $1.5 \times 10^{-3}$  Pa) and  $5 \times 10^{15} \text{ m}^{-3}$  (at 90 deg at a backpressure of  $4.8 \times 10^{-4}$  Pa), a difference in the random ion flux current density to the presheath before the Bohm velocity criterion is applied can be estimated. The

thermal velocity of the xenon ions is approximately 232 m/s at 425 K. With these parameters, the difference in the random flux current is estimated to be  $4.6 \times 10^{-3} \text{ mA/cm}^2$ . For the test cases chosen, the measured difference between ion current density measurements for different backpressures at 90 deg is approximately  $3.9 \times 10^{-3} \text{ mA/cm}^2$ . The estimated increase in current density from thermal ions and the measured difference in current densities for different background pressures are within 20% of each other. This concurs with the theory that thermal ions created from CEX at higher background pressures increase current density measurements at angles beyond 40 deg from the thruster centerline.

## Conclusions

The ion current density distribution of the 173Mv1 Hall thruster at typical operating conditions is measured with a nude Faraday probe. The magnitude of the ion current density in the plume increases at large angles from the thruster centerline with increasing facility background pressure because the Faraday probe collects CEX ions. The Langmuir probe measurements show a weak electric field near the Faraday probe that is confined to within a few centimeters of the probe face. The magnitude of this electric field is not strong enough to affect CEX or discharge ion collection by the probe surface significantly.

## Acknowledgments

The research contained herein was sponsored by the U.S. Air Force Office of Scientific Research (Mitat Birkan, Contract Monitor). We would like to thank Colleen Marrese at the Jet Propulsion Laboratory, California Institute of Technology for lending the Plasma Dynamics and Electric Propulsion Laboratory (PEPL) the nude Faraday probes, Robert Jankovsky at NASA John H. Glenn Research Center at Lewis Field for lending PEPL the laboratory-model hollow cathode, the Moscow Aviation Institute for lending PEPL the laboratory-model cathode, Terry Larrow for fabricating the hardware used in this study, and the departmental technical staff and other graduate students at PEPL for help in maintaining the facilities. M. Walker is supported by the Michigan Space Grant Consortium and the National Science Foundation. A. Victor is supported by the Michigan Space Grant Consortium as well as the University of Michigan Aerospace Engineering Department. R. Hofer is supported by the NASA Graduate Student Research Program. The authors are greatly appreciative of this support.

## References

- Sankovic, J. M., Hamley, J. A., and Haag, T. W., "Performance Evaluation of the Russian SPT-100 Thruster at NASA LaRC," *Proceedings of the International Electric Propulsion Conference*, Paper IEPC-93-094, Electric Rocket Propulsion Society, Sept. 1993.
- Garner, C. E., Brophy, J. R., Polk, J. E., and Pless, L. C., "A 5,730-Hr Cyclic Endurance Test of the SPT-100," AIAA Paper 95-2667, July 1995.
- Hargus, W., Jr., Fife, J. M., Mason, L., Jankovsky, R., Haag, T., Pinerio, L., and Snyder, J. S., "Preliminary Performance Results for the High Performance Hall System SPT-140," AIAA Paper 2000-3250, July 2000.
- Fife, J. M., Hargus, W., Jr., Jaworske, D. A., Sarmient, C., Mason, L., Jankovsky, R., Snyder, J. S., Malone, S., Haas, J., and Gallimore, A., "Spacecraft Interaction Test Results of the High Performance Hall System SPT-140," AIAA Paper 2000-3521, July 2000.
- Pollard, J. E., Diamante, K. D., Khayms, V., Werthman, L., King, D. Q., and de Grys, K. H., "Ion Flux, Energy, and Charge-State Measurements for the BPT-4000 Hall Thruster," AIAA Paper 2001-3351, July 2001.
- Mason, L. S., Jankovsky, R. S., and Manzella, D. H., "1000 Hours of Testing on a 10 Kilowatt Hall Effect Thruster," AIAA Paper 2001-3773, July 2001.
- Britt, N., "Overview of EP in U.S. Industry," AIAA Paper 2002-3559, July 2002.
- Jankovsky, R. S., Jacobson, and Manzella, D. H., "50 kW Class Krypton Hall Thruster Performance," AIAA Paper 2003-4550, July 2003.
- Beal, B. E., Gallimore, A. D., and Hargus, W., Jr., "Effects of Clustering Multiple Hall Thrusters on Plasma Plume Properties," AIAA Paper 2003-5155, July 2003.
- King, L. B., Gallimore, A. D., and Marrese, C. M., "Transport-Property Measurements in the Plume of an SPT-100 Hall Thruster," *Journal of Propulsion and Power*, Vol. 14, No. 3, 1998, pp. 327–335.

- <sup>11</sup>Semenkin, A., Kim, V., Gorshkov, O., and Jankovsky, R., "Development of Electric Propulsion Standards—Current Status and Further Activity," *Proceedings of the International Electric Propulsion Conference*, Paper IEPC-01-070, Electric Rocket Propulsion Society, Oct. 2001.
- <sup>12</sup>Hofer, R. R., Peterson, P. Y., and Gallimore, A. D., "Characterizing Vacuum Facility Backpressure Effects on the Performance of a Hall Thruster," *Proceedings of the International Electric Propulsion Conference*, Paper IEPC-01-045, Electric Rocket Propulsion Society, Oct. 2001.
- <sup>13</sup>Hofer, R. R., Walker, M. L. R., and Gallimore, A. D., "A Comparison of Nude and Collimated Faraday Probes for Use with Hall Thrusters," *Proceedings of the International Electric Propulsion Conference*, Paper IEPC-01-20, Electric Rocket Propulsion Society, Oct. 2001.
- <sup>14</sup>de Grys, K. H., Tilley, D. L., and Aadland, R. S., "BPT Hall Thruster Plume Characteristics," AIAA Paper 99-2283, June 1999.
- <sup>15</sup>Walker, M. L. R., Gallimore, A. D., Cai, C., and Boyd, I. D., "Pressure Map of a Facility as a Function of Flow Rates to Study Facility Effects," AIAA Paper 2002-3815, July 2002.
- <sup>16</sup>Randolph, T., Kim, V., Kaufman, H., Kozubsky, K., Zhurin, V., and Day, M., "Facility Effects on Stationary Plasma Thruster Testing," *Proceedings of the International Electric Propulsion Conference*, Paper IEPC-93-93, Electric Rocket Propulsion Society, Sept. 1993.
- <sup>17</sup>Dushman, S., *Scientific Foundations of Vacuum Technique*, Vol. 4, Wiley, New York, 1958.
- <sup>18</sup>Haas, J. M., "Low-Perturbation Interrogation of the Internal and Near-field Plasma Structure of a Hall Thruster Using a High-Speed Probe Positioning System," Ph.D. Dissertation, Dept. of Aerospace Engineering, Univ. of Michigan, Ann Arbor, MI, Feb. 2001, pp. 176–186.
- <sup>19</sup>Haas, J. M., Gulczinski, F. S., and Gallimore, A. D., "Performance Characteristics of a 5 kW Laboratory Hall Thruster," AIAA Paper 98-3503, July 1998.
- <sup>20</sup>Hofer, R. R., Peterson, P. Y., and Gallimore, A. D., "A High Specific Impulse Two-Stage Hall Thruster with Plasma Lens Focusing," *Proceedings of the International Electric Propulsion Conference*, Paper IEPC-01-036, Electric Rocket Propulsion Society, Oct. 2001.
- <sup>21</sup>Hofer, R. R., and Gallimore, A. D., "Role of Magnetic Field Topography in Improving the Performance of a High Voltage Hall Thruster," AIAA Paper 2002-4111, July 2002.
- <sup>22</sup>Sarver-Verhey, T. R., "28,000 hour Xenon Hollow Cathode Life Test Results," International Electric Propulsion Conference, Paper IEPC-97-168, Aug. 1997.
- <sup>23</sup>Brown, S. C., *Basic Data of Plasma Physics*, McGraw-Hill, New York, 1959.
- <sup>24</sup>Manzella, D. H., and Sankovic, J. M., "Hall Thruster Ion Beam Characterization," AIAA Paper 95-2927, July 1995.
- <sup>25</sup>*Handbook of Plasma Diagnostics*, Hidden Analytical, Ltd., 2000.
- <sup>26</sup>Hutchinson, I. H., *Principles of Plasma Diagnostics*, Cambridge Univ. Press, New York, 1987.
- <sup>27</sup>Gulczinski, F. S., "Examination of the Structure and Evolution of Ion Energy Properties of a 5 kW Class Laboratory Hall Effect Thruster at Various Operational Conditions," Ph.D. Dissertation, Dept. of Aerospace Engineering, Univ. of Michigan, Ann Arbor, MI, Aug. 1999, pp. 72–80.
- <sup>28</sup>Boyd, I. D., and Dressler, R. A., "Far Field Modeling of the Plasma Plume of a Hall Thruster," *Journal of Applied Physics*, Vol. 92, No. 4, 2002, p. 1764.
- <sup>29</sup>Williams, G. J., Smith, T. B., Gulczinski, F. S., and Gallimore, A. D., "Correlating Laser-Induced Fluorescence and Molecular Beam Mass Spectrometry Ion Energy Distributions," *Journal of Propulsion and Power*, Vol. 18, No. 2, 2002, pp. 489–491.